Precision Control of a Piezoceramic Actuator Using Neural Networks

Ying-Shieh Kung
Department of Electrical Engineering
Southern Taiwan University of Technology

No.1 Nan-Tai Street, Yung-Kang, Tainan Hsien
Taiwan, 710, R.O.C.
kung@mail.stut.edu.tw

Rong-Fong Fung
Department of Mechanical and Automation Engineering
National Kaohsiung First University of Science and Technology
No.2 Jou-Ye Road, Nan-Tzo, Kaohsiung,
Taiwan, 824, R.O.C.
rffung@ccms.nkfust.edu.tw

***Abstract* –This paper is to study the precision control of a piezoceramic actuator (PA). Due to the inherent hysteresis nonlinearity, the PA always causes position error in the open-loop system and instability in the closed-loop system. To remedy this problem, a new control method combining the feedforward and feedback controllers is proposed to improve the dynamic performance of the PA. In the feedforward controller design, the hysteresis nonlinearity of the PA is modeled by using Preisach model first. A database of input/output history and a neural networks architecture treated as the inverse function of Preisach model are also utilized in the feedforward controller. In the feedback controller design, a PI controller is used to regulate the error between the command input and system output. In experiment, the command of square wave, sinusoid wave and triangular wave is taken as the tested signal to validate the excellent performances of the proposed controller.**

I. INTRODUCTION

Piezoceramic actuators, in Fig. 1, with many advantages such as high stiffness, fast-frequency response and nanometer resolution [1] have been used in many applications that require precise positioning control in recent years. Application examples include scanning tunneling microscope [2], stepper, diamond turning machine, positioning lenses and mirrors in optical systems [3], and etc. However, piezoceramic materials also have the following drawbacks [1] of the mechanical properties, such as, non-linearity, hysteresis, creep and thermal variations. These drawbacks, especially the effect of hysteresis, often cause the positioning error and diminish the performance quality of machine equipment in the open-loop system. In order to solve these problems, there have been amounts of research efforts in the past. Newcomb and Flinn [4] proposed a linear control technique by use of the charge instead of voltage as control input. Although its hysteresis effect and linear relationship are apparently improved, it decreases the frequency of response. Jung and Kim [5] presented a feedforward control method to improve the scanning accuracy of a scanning tunneling microscope. However, it could not completely express the dynamic behavior of the PA because its hysteresis nonlinearity only considers the symmetry and local memory. In order to improve the dynamic performance of the PA, a new control method including the feedforward and feedback controllers is designed. The feedforward controller contains a database of input/output history and the neural network architecture to replace the inverse function of Preisach model. The feedback PI controller is used to increase the positioning accuracy of the PA. By using the neural networks technique [6] to model the inverse function of Preisach model, the hysteresis behavior is improved, the position control is more accuracy, and the command tracking becomes faster response in the experiments.

II. MATHEMATICAL MODEL FOR THE PIEZOCERAMIC HYSTERESIS

The classical Preisach model [7] used to model the nonlinear hysteresis behavior of the PA is described as

$$y(t) = \iint_{\alpha \geq \beta} \mu(\alpha, \beta)\gamma_{\alpha\beta}[u(t)]d\alpha d\beta \qquad (1)$$

where $y(t)$ is the output response of the PA; $\mu(\alpha,\beta)$ is a weighing function of Preisach model; α and β correspond to "up" and "down" switching values of the inputs, respectively; and $\gamma_{\alpha\beta}[u(t)]$ is similar to a two-position relay and represents a hysteresis operator, whose value is determined by α , β and input $u(t)$.When the input $u(t)$ is larger than α , $\gamma_{\alpha\beta}[u(t)]$ is switched to the "up" position, and when the input $u(t)$ is less than β , $\gamma_{\alpha\beta}[u(t)]$ is switched to the "down" position. The input value $u(t)$ of the PA could be divided into two conditions: the monotonically increasing and decreasing conditions [8]. The former condition corresponds to the ascending branches of hysteresis loops in Fig. 2, where the input of the PA changes from $\beta_0 \to \alpha_1 \to \beta_1 \to \alpha_2 \to \beta_2 \to u(t)$. The output displacement y(t) is the sum of double integral of the weighing function $\mu(\alpha,\beta)$ on the trapezoidal regions of R^+ in Fig. 3. The $\gamma_{\alpha\beta}[u(t)]$ value is 1 in the region $R^+(t)$ and is 0 out of the region $R^+(t)$. Therefore, (1) can be simplified as (2).

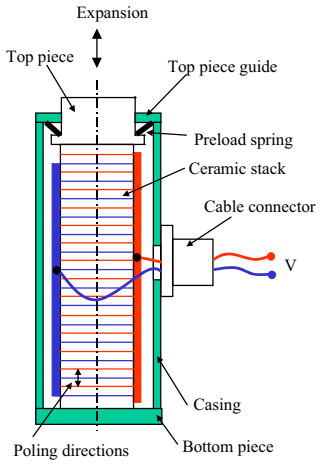

Fig. 1. Piezoceramic Actuator

0-7803-7474-6/02/$17.00 ©2002 IEEE

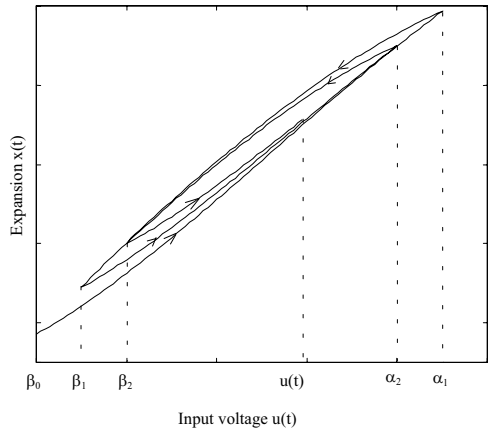

Fig. 2. The hysteresis loop of the PA with ascending branch

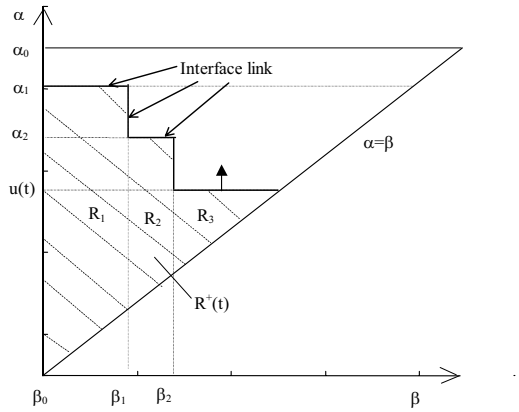

Fig. 3. The region $R^+(t)$ corresponds to the hysteresis loop shown in Fig. 2

$$y(t) = \iint_{R^+(t)} \mu(\alpha,\beta)\, d\alpha\, d\beta$$
$$= \left(\iint_{R_1(t)} + \iint_{R_2(t)} + \iint_{R_3(t)}\right) \mu(\alpha,\beta) d\alpha\, d\beta \quad (2)$$
$$\triangleq [X(\alpha_1,\beta_0) - X(\alpha_1,\beta_1)] + [X(\alpha_2,\beta_1) - X(\alpha_2,\beta_2)] + X(u(t),\beta_2),$$

or, in general

$$y(t) = \sum_{k=1}^{N} [X(\alpha_k,\beta_{k-1}) - X(\alpha_k,\beta_k)] + X(u(t),\beta_N) \quad (3)$$
$$\triangleq y_H + y_C,$$

where

$$X(\alpha,\beta) = \iint_{R(\alpha,\beta)} \mu(\alpha,\beta)\, d\alpha\, d\beta, \quad (4)$$

is defined as Preisach function representing the change in output $y(t)$ as the input $u(t)$ changes from α to β; $y_H \triangleq \sum_{k=1}^{N} [X(\alpha_k,\beta_{k-1}) - X(\alpha_k,\beta_k)]$ is defined as the sum of output displacements for several switching input histories, and $y_c \triangleq X(u(t),\beta_N)$ is defined as the output displacement for current input on the ascending branch. Similarly, for the latter condition corresponds to the descending branches of hysteresis loops, if the input of the PA changes from $\beta_0 \to \alpha_1 \to \beta_1 \to \alpha_2 \to \beta_2 \to \alpha_3 \to u(t)$, (1) can also be simplified as

$$y(t) = \iint_{R^+(t)} \mu(\alpha,\beta)\, d\alpha\, d\beta$$
$$= \left(\iint_{R_1(t)} + \iint_{R_2(t)} + \iint_{R_3(t)}\right) \mu(\alpha,\beta) d\alpha\, d\beta \quad (5)$$
$$\triangleq [X(\alpha_1,\beta_0) - X(\alpha_1,\beta_1)] + [X(\alpha_2,\beta_1) - X(\alpha_2,\beta_2)] + [X(\alpha_3,\beta_2) - X(\alpha_3,u(t))],$$

or, in general

$$y(t) = \sum_{k=1}^{N-1} [X(\alpha_k,\beta_{k-1}) - X(\alpha_k,\beta_k)] + [X(\alpha_N,\beta_{N-1}) - X(\alpha_N,u(t))] \quad (6)$$
$$\triangleq y_H + y_C,$$

where $y_H \triangleq \sum_{k=1}^{N-1} [X(\alpha_k,\beta_{k-1}) - X(\alpha_k,\beta_k)] + X(\alpha_N,\beta_{N-1})$, and $y_C \triangleq -X(\alpha_N,u(t))$.

Equations (3) and (6), and the experimental data in Fig. 2, all show that the hysteresis behave of the PA is 'non-local memory' because the current output displacement of the PA depends not only upon the current input but also upon the past several switching inputs. Basically, Preisach function X(α,β) in (3) and (6) can be obtained from the reversal curves of expansion displacements in experiments as shown in Fig. 4.

III. CONTROLLER DESIGN OF THE PA WITH THE NEURAL NETWORKS

To cope with the nonlinear hysteresis problem of the PA, a control algorithm combining the feedforward and feedback controllers is presented in Fig. 5. The new feedforward controller using the neural networks is designed to obtain the inverse function of Preisach model in (1) for the purpose that the multiplication of the transfer function of PA and the feedforward controller could approaches 1. A feedback controller constructed by the PI controller is to compensate the error between the input command and output displacement of the PA. Referring to (3) and (6), the feedforward controller in Fig. 5 can be established according to the input being in the monotonically increasing or decreasing conditions.

1. <u>In the monotonically increasing condition</u>:

From (3), let the output displacement of the PA be equal to the input command, y = r, and yield (7).

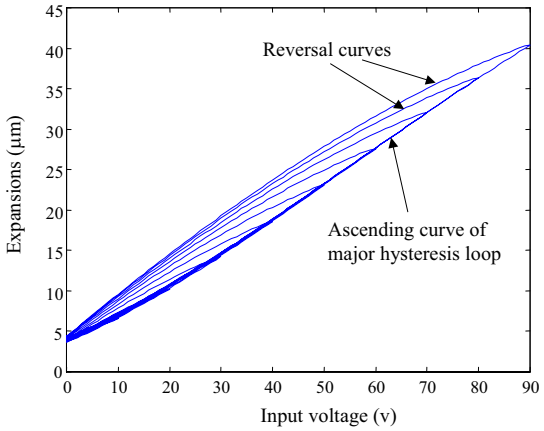

Fig. 4. The reversal curves of expansion displacements of the PA

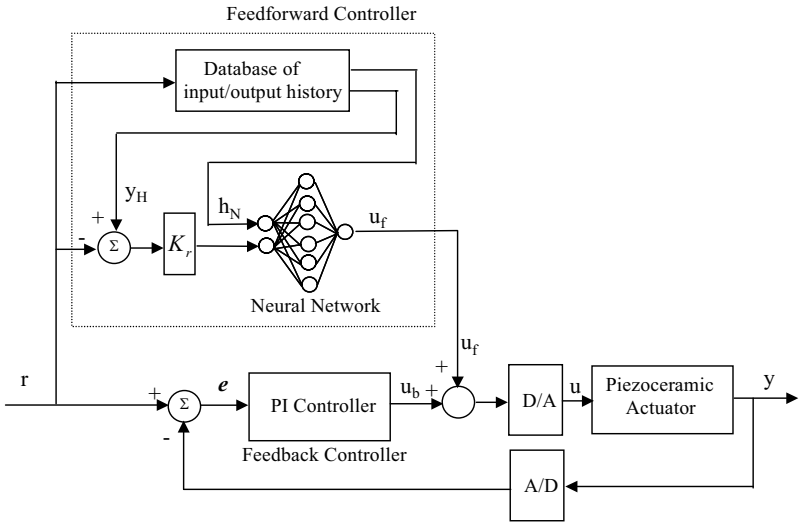

Fig. 5. The neural networks feedforward and PI feedback controllers

$$\mathrm{X}(u_f(t),\beta_N) = r(t) - \sum_{k=1}^{N}[\mathrm{X}(\alpha_k,\beta_{k-1}) - \mathrm{X}(\alpha_k,\beta_k)] \quad (7)$$
$$\triangleq r(t) - y_H.$$

Therefore, the control effort of the feedforward controller is given as follows:

$$u_f(t) = X^{-1}(\beta_N, r(t) - y_H), \quad (8)$$

where $X^{-1}(.)$ denotes the inverse Preisach function which is replaced by a three-layer feedforward neural networks. The inputs of $X^{-1}(.)$ or the neural networks are β_N and $r(t) - y_H$, the output is $u_f(t)$, and y_H is the sum of the output displacements for the past switching input history. Therefore, from (8), the parameters in Fig. 5 are K_r = -1, $h_N = \beta_N$ and

$$y_H = \sum_{k=1}^{N}[\mathrm{X}(\alpha_k,\beta_{k-1}) - \mathrm{X}(\alpha_k,\beta_k)].$$

2. <u>In the monotonically decreasing condition</u>:

From (6) and the same condition in the previous section, we have

$$\mathrm{X}(\alpha_N, u_f(t)) = \sum_{k=1}^{N-1}[\mathrm{X}(\alpha_k,\beta_{k-1}) - X(\alpha_k,\beta_k)] \quad (9)$$
$$+ \mathrm{X}(\alpha_N,\beta_{N-1}) - r(t) \triangleq y_H - r(t).$$

The control effort of the feedforward controller is given as follows:

$$u_f(t) = X^{-1}(\alpha_N, y_H - r(t)), \quad (10)$$

The inputs of $X^{-1}(.)$ or the neural networks are α_N and $y_H - r(t)$, and the output is $u_f(t)$. Therefore, from (10), the parameters in Fig. 5 are $K_r = 1$, $h_N = \alpha_N$ and

$$y_H = \sum_{k=1}^{N-1}[\mathrm{X}(\alpha_k,\beta_{k-1}) - X(\alpha_k,\beta_k)] + \mathrm{X}(\alpha_N,\beta_{N-1}).$$

The inverse Preisach function $\mathrm{X}^{-1}(\alpha,\beta)$ in (8) and (10) is replaced by a three-layer feedforward neural-networks and the procedure of the forward computation for the neural networks is as follows.

① The input of node j at layer k:

The first layer (k=1):

$$I_1^1 = h_N, \quad I_2^1 = K_r * (y_H - r(t)), \quad (11)$$

where I_j^1 is the input of the *j*th node at first layer. The number of nodes is n_1=2.

The second and third layers (k=2 and 3):

$$I_j^k \triangleq net_j = \sum_{i=0}^{n_{k-1}} W_{ji}^k O_i^{k-1}, \quad \mathrm{j}=1,2,..,n_k, \quad (12)$$

where O_i^k denotes the output of the *i*th node at layer k, O_0^k is the bias node of layer k, W_{ji}^k is the connection weight from the *i*th node at layer k-1 to the *j*th node at layer k and n_K is the number of nodes at layer k. In the third layer, the number of nodes is $n_3 = 1$.

② The output of node j at layer k, (k=2,3):

$$O_j^k = f(I_j^k), \quad \mathrm{j} = 1,2,..., n_k, \quad (13)$$

where f(•) is an activation function which is a sigmoidal function as:

$$O_j^k = \frac{1}{1 + e^{-(I_j^k + \eta_j)/\eta_0}}, \quad (14)$$

where η_i is a threshold or bias and η_0 is used to modify the shape of the sigmoid.

The output vector is equal to the input vector for the first layer, that is, $O_1^1 = I_1^1$, $O_2^1 = I_2^1$ and the output from the third layer is $u_f = O_1^3$.

The net connection weights, W_{ji}^k, in the networks can be determined according to the following training procedure:

① Set the possible input voltage range during operation as:

$$u_{\min} \le u \le u_{\max}. \quad (15)$$

② Within the range of (15), *u* is divided into M sets with a fixed step size (corresponding to the value of α_i, i=1, 2,..., M), and the voltage-displacement data pairs [α_i, y_i] can be

collected from the ascending curves of major hysteresis loop in Fig. 4. In similarity, for each reversal curve, voltage-displacement data pairs $[\beta_j, y_j]$, j=1, 2,..., m_i, can also be collected. Therefore, the output value of Preisach function from switching input voltage α_i to β_j in each reversal curve can be obtained by calculating $X(\alpha_i,\beta_j) = y_i - y_j$. For all reversal curves in Fig. 4, the total collected data can be rearranged by two data sets. One data set has the input vector $\mathbf{Q}_1 = [\alpha_i, X(\alpha_i,\beta_j)]$ and the output vector $\mathbf{Y}_1 = [\beta_j]$, and the other data set has the input vector $\mathbf{Q}_2 = [\beta_i, X(\alpha_i,\beta_j)]$ and the output vector $\mathbf{Y}_2 = [\alpha_j]$ with i=1, 2,…, M and j=1, 2,..., m_i. The total number of data sets is N=2$\sum_{i=1}^{M} m_i$, where m_i is the number of collected data for each reversal curve. The relation between input and output vectors can be regarded as a mapping problem of Y=f(Q), ($Q \in R^n$, n=2, $Y \in R^m$, m=1) and it is possible to closely approximate this map via a neural net learning [6].

③ From the above known data pairs $\{(\mathbf{Q}_1^i, \mathrm{Y}_1^i)$, i=1,2,…N/2$\}$ and $\{(\mathbf{Q}_2^i, \mathrm{Y}_2^i)$, i=1,2,…N/2$\}$, the connection weights W_{ji}^k, k=2, 3, which denote the connection from the *i*th node at layer k-1 to the *j*th node at layer k, are found using the backpropagation learning algorithm [6]. Once the connection weights W_{ji}^k of a three-layer feedforward neural network are obtained, the control effort can be derived on line through the feedforward computation of the neural networks as shown in Fig.5.

A PI controller in Fig.5 is adopted as a feedback controller for the purpose of compensating the system uncertainty, load disturbance or mapping error of the neural networks. The digital PI control algorithm is given by

$$u_b(z^{-1}) = K_P\, e(z^{-1}) + \frac{K_I z^{-1}}{1 - z^{-1}} e(z^{-1}), \qquad (16)$$

where z^{-1} is the back shift operator, and K_P, K_I are proportional and integral gains, respectively.

IV. EXPERIMENTS AND RESULTS

The block diagram of the proposed control system is shown in Fig. 5, which consists of a PA, a position sensor, a power amplifier, an 12-bit A/D-D/A converter interface card and a computer. The PA model is P-841.30 made by Physik Instrumente[3], and has a nominal expansion of 0~45μm under an input voltage of 0~100V. A position sensor of strain gauge attached to the PA has a linear resolution of 0.1~0.2%. The experimental results of hysteresis phenomenon of the P-841.30 PA are shown in Fig. 2. For constructing the neural networks to replace the inverse Preisach function of the control mode in Fig. 5, the voltage-displacement data pairs are collected and stored in computer via the A/D-D/A interface card. In our experiments, the voltage-displacement data pairs for 9 reversal curves (descending curves) of the ascending curves of major hysteresis loop in Fig. 4 are collected. These reversal curves correspond 9 values of α_i with 10V, 20V,..., 90V. For each reversal curve with α_i, some points from α_i to 0 corresponding to the value of β_j with fixed step size of 1V are collected. For example, the 91 values of β_j with 90V, 89V,…, 1V, 0V for the largest reversal curve (α_i =90V), or 11 values of β_j with 10V, 9V,..., 0V for the smallest reversal curve (α_i =10V) are collected.

In the control mode, using the collected voltage-displacement data pairs, we arrange it in the form that the input vector is Q=$\begin{bmatrix} Q_1 \\ Q_2 \end{bmatrix}$, the output vector is Y=$\begin{bmatrix} \mathrm{Y}_1 \\ \mathrm{Y}_2 \end{bmatrix}$ with $Q_1=[\alpha_i, X(\alpha_i,\beta_j)]$, $Q_2=[\beta_i, X(\alpha_i,\beta_j)]$, $\mathrm{Y}_1=[\beta_j]$, $\mathrm{Y}_2=[\alpha_j]$, i=1, 2,..., 9, j=1, 2, ..., m_I, and where $X(\alpha_i,\beta_j) = y_i - y_j$. The total number of data sets is N=2*$\sum_{i=1}^{M} m_i$ =2*(91+81+...,11) =918. In Fig. 5, these data pairs are used to train the connection weights W_{ji}^k in the neural networks and to replace the inverse Preisach function $X^{-1}(\alpha_i,\beta_j)$ in (8) and (10). In the implementations, to validate the effectiveness of the proposed controller, an input command of 10 Hz square wave with amplitudes of 9 μm and 36 μm in Fig. 5 is used to test the performances of the output responses and the controller schemes of the PI feedback controller only (regular PI controller), the neural networks feedforward controller only (NN controller alone) and the neural networks feedforward controller plus PI feedback controller (NN+PI controller), respectively. The sampling frequency of the control loop is 2 kHz and the output responses in different controller schemes are shown in Figs. 6~7. Fig. 6 shows that the effect of hysteresis phenomenon causes a large asymmetric steady-state error in the open-loop actuator system, but the proposed controller (NN+PI controller) has a good command tracking with 2 ms rising time, 2.5 ms settling time and zero steady-state error. Fig. 7 shows that in the case of the NN controller alone, it has a steady-state error with 0.45 μm at 36 μm position command input or 0.09 μm at 9 μm position command input. In the case of the regular PI controller, its response is slower than the other two controllers and has a little oscillation in transient state. Only the proposed NN+PI controller has the best characteristics with fast command regulation and zero steady-state error. To further compare the tracking control performance among the regular PI controller, the NN controller alone and the NN+PI controller, the input signals using the sinusoid wave with a amplitude of 27 μm (bias 22.5 μm) and different signal frequencies for 20 and 100 Hz were employed. The tracking results are plotted in Figs. 8~9. In the low-frequency tracking, such as a 20 Hz sine wave of the input command, three control schemes shown in Fig. 8 all have a good command tracking. In a higher-frequency tracking, such as the 100 Hz sine wave of input command, Fig. 9 shows that the NN+PI controller possesses a low decay value and a smaller tracking error than that of the regular PI controller. It demonstrates that the proposed controller have a

good tracking accuracy in high-frequency response. To test

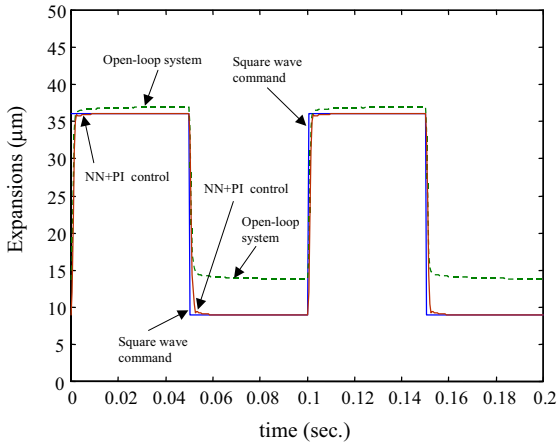

Fig. 6. Output responses of an open-loop system and the proposed NN+PI controller

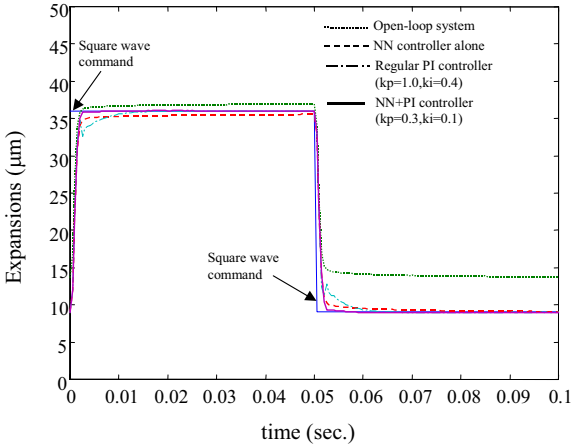

Fig. 7. Comparing the output responses of different control schemes

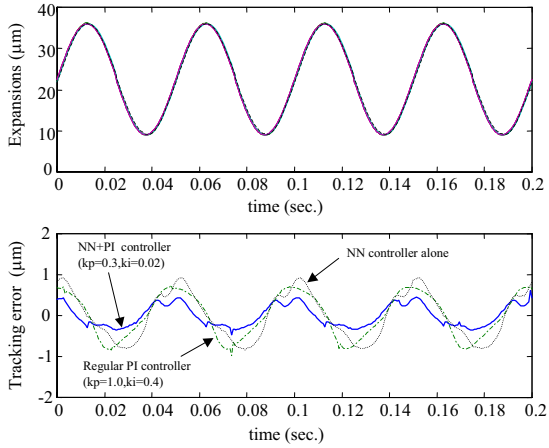

Fig. 8. The tracking results of different controllers with a 20Hz sinusoid input signal

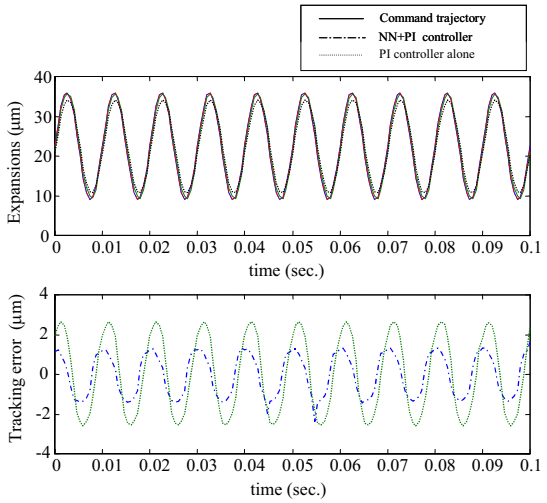

Fig. 9. Comparison of a regular PI controller and a NN+PI controller for tracking a 100Hz sinusoid input signal

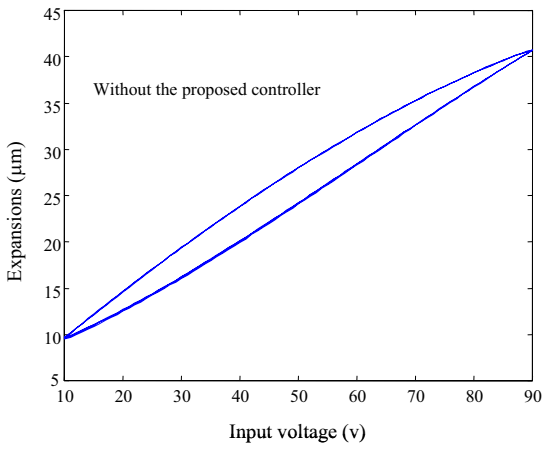

(a)

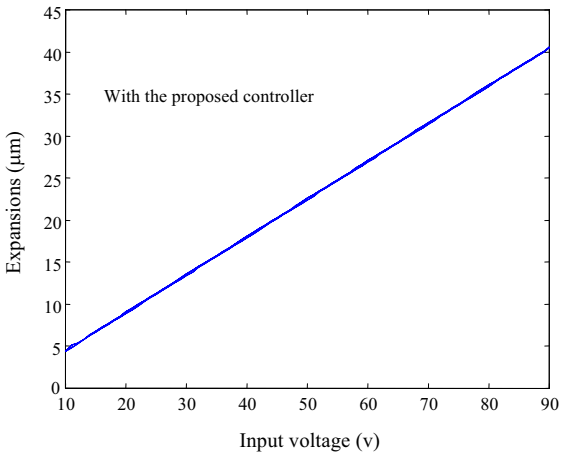

(b)

Fig. 10. (a) The hysteresis phenomenon in the open-loop control. (b) The linear result is improved by the proposed controller.

the hysteresis ratio, the input signals using the triangular wave with a amplitude of 36 μm and a frequency of 10 Hz are employed. It is shown in Fig. 10 that the hysteresis ratio is decreased from a open-loop system with a maximum deviation 17% to a proposed closed-loop control system with a maximum one 0.8%.

V. CONCLUSIONS

A controller based on the neural network technique for the PA has been presented. In controller design, an architecture with both feedforward and feedback controllers is adopted. The feedforward controller is used for the inverse function of Preisach model and the feedback controller is used to regulate the errors between the input commands and output responses. From experimental results, the output expansions can track input commands perfectly, and the nonlinear hysteresis phenomenon can be improved well. The effectiveness of the proposed controller is then confirmed.

VI. ACKNOWLEDGMENT

This work was supported by National Science Council of the R.O.C. under grant no. NSC-89-2213-E-218-019.

VII. REFERENCES

[1] T. G. King, M. E. Preston, B. J. M. Murphy and D. S. Cannell, “Piezoelectric Ceramic Actuators: A Review of Machinery Applications,” *Precision Engineering*, vol. 12, no. 3, 1990, pp. 131-136.

[2] D. Sarid, *Scanning Force Mocroscopy-with Applications to Electric, Magnetic and Atomic Forces*, New York Oxford, 1991.

[3] Insrumente Physik, *Products for Micro-positioning Catalogue*, Edition E, 2000.

[4] C. Newcomb and I. Flinn, “Improving the Linearity of Piezoelectric Ceramic Actuators,” *Electronics Letters*, vol. 18, no. 11, 1982, pp. 442-444.

[5] S. Jung and S. Kim, “Improvement of Scanning Accuracy of PZT Piezoelectric Actuators by Feedforward Model-reference Control,” *Precision Engineering*, vol. 16, no. 1, 1994, pp. 49-55.

[6] J. C. Principe, N. R. Euliano, *Neural and Adaptive Systems – Fundamentals Through Simulations*, John Wiley & Sons, Inc. 2000.

[7] I. Mayergoyz, *Mathematical Models of Hysteresis*, New York: Springer-Verlag, 1991.

[8] P. Ge and M. Jouaneh, “Modeling Hysteresis in Piezoceramic Actuators,” *Precision Engineering*, vol. 17, no.3, 1995, pp.211-221.